Brain Structure and Function (2019) 224:2717–2731
https://doi.org/10.1007/s00429-019-01929-2

ORIGINAL ARTICLE

Short-term plasticity after partial deafferentation in the oculomotor system

Rosendo G. Hernández[1] · Souhail Djebari[1] · José Miguel Vélez-Ortiz[1] · Rosa R. de la Cruz[1] · Angel M. Pastor[1] · Beatriz Benítez-Temiño[1]

Received: 31 January 2019 / Accepted: 26 July 2019 / Published online: 2 August 2019

Abstract

Medial rectus motoneurons are innervated by two main pontine inputs. The specific function of each of these two inputs remains to be fully understood. Indeed, selective partial deafferentation of medial rectus motoneurons, performed by the lesion of either the vestibular or the abducens input, initially induces similar changes in motoneuronal discharge. However, at longer time periods, the responses to both lesions are dissimilar. Alterations on eye movements and motoneuronal discharge induced by vestibular input transection recover completely 2 months post-lesion, whereas changes induced by abducens internuclear lesion are more drastic and permanent. Functional recovery could be due to some kind of plastic process, such as reactive synaptogenesis, developed by the remaining intact input, which would occupy the vacant synaptic spaces left after lesion. Herein, by means of confocal microscopy, immunocytochemistry and retrograde labeling, we attempt to elucidate the possible plastic processes that take place after partial deafferentation of medial rectus motoneuron. 48 h post-injury, both vestibular and abducens internuclear lesions produced a reduced synaptic coverage on these motoneurons. However, 96 h after vestibular lesion, there was a partial recovery in the number of synaptic contacts. This suggests that there was reactive synaptogenesis. This recovery was preceded by an increase in somatic neurotrophin content, suggesting a role of these molecules in presynaptic axonal sprouting. The rise in synaptic coverage might be due to terminal sprouting performed by the remaining main input, i.e., abducens internuclear neurons. The present results may improve the understanding of this apparently redundant input system.

Keywords Oculomotor · Synaptic plasticity · Motoneuron · Neurotrophins

Introduction

Medial rectus motoneurons are located at the oculomotor nucleus. These innervate the ipsilateral medial rectus muscle, whose action moves the eye nasally. Medial rectus motoneuronal firing is driven by two main pontine inputs: (1) the abducens internuclear neurons, located in the abducens nucleus, whose axons cross the midline at the level of the abducens nucleus, course through the medial longitudinal fascicle (MLF) and terminate on the contralateral medial rectus motoneurons (Biefang 1978; Highstein and Baker 1978; Carpenter and Carleton 1983); and (2) the second-order vestibular neurons located in the ipsilateral lateral vestibular nucleus, which reach the oculomotor complex through the ascending tract of Deiters (ATD; Baker and Highstein 1978; Reisine and Highstein 1979; Furuya and Markham 1981). This dual input system on medial rectus motoneurons plays an important role for conjugating the movements of both eyes in the horizontal plane (Delgado-García et al. 1986). The lateral vestibular nucleus carries information related to head velocity, while the abducens internuclear neurons inform medial rectus motoneurons about information of eye velocity and position in horizontal gaze (Baker and Highstein 1978; Furuya and Markham 1981; Reisine et al. 1981). However, while abducens internuclear neurons receive afferents from many premotor areas and exhibit a firing pattern that resembles that of their neighboring lateral rectus motoneurons, encoding eye position and velocity signals (Delgado-García et al. 1986), lateral

Rosendo G. Hernández and Souhail Djebari are co-first authors.

✉ Angel M. Pastor
ampastor@us.es

[1] Departamento de Fisiología, Universidad de Sevilla, Avda. Reina Mercedes, 6, 41012 Seville, Spain

vestibular neurons receive direct sensory vestibular inputs and display mainly a head velocity signal with a weak eye position and velocity component (Reisine et al. 1981).

In addition, the somatodendritic distribution of these two inputs on medial rectus motoneurons is anatomically segregated. While vestibular terminals end mainly on motoneuron somata and proximal dendrites, abducens internuclear neuron terminals are located preferentially on more distal dendrites (Nguyen et al. 1999). The role of these two excitatory inputs might be modulated by inhibitory signals, whose origin remains to be fully understood, but might correspond, at least in part, to local oculomotor interneurons (de la Cruz et al. 1992). Other inputs to medial rectus motoneurons arise from the mesencephalic reticular formation (Bohlen et al. 2017), some of which carry vergence signals (Zhang et al. 1991), and from the superior colliculus (Izawa et al. 1999) and prepositus hypoglossi nucleus (McCrea and Baker 1985).

According to the literature, thus, extraocular motoneurons, as many other motor neurons, receive different inputs carrying segregated signals that, once integrated, define a unified firing pattern that encodes muscle contraction (Büttner-Ennever 2006). However, medial rectus motoneurons represent an example of motoneurons that receive an already integrated, and apparently duplicated, signal. Whether this dual afferent system is indeed redundant, or instead, both inputs subserve different functions, remains to be fully clarified. In this context, we were interested in elucidating plastic changes in this circuitry, which is involved in conjugate horizontal gaze, after the selective lesion of each tract.

We have previously shown that partial deafferentation of medial rectus motoneurons, achieved by the transection of either the MLF or the ATD, induces motor changes in the movement of the ipsilateral eye, as well as a reduction in motoneuronal sensitivity to eye position and velocity, during both spontaneous and vestibular reflex eye movements. However, this effect is more drastic after MLF than after ATD transection in spite of the vestibular nature of the ATD projection (Hernández et al. 2017a). Given the similar qualitative consequences of MLF or ATD deprivation, it could be concluded that none of these routes can be replaced by the other. Thus, rather than being redundant, they could be considered complementary, and both would be necessary for the eyes to display a proper horizontal gaze coordination.

Vestibular lesions have transitory effects, while changes produced by MLF transection are permanent. The recovery described after ATD transection could be due, on one side, to an increase in motoneuron excitability, as described previously in deafferented second-order vestibular neurons (Him and Dutia 2001), and on the other side, to a process of reactive synaptogenesis performed by the remaining (intact) input, the abducens internuclear projection. This second hypothesis seems more plausible, since a rise in synaptic coverage has already been described in this system 2 months after partial deafferentation, when compared with data obtained 3 days after lesion (Hernández et al. 2017a). However, the time course of this plastic process remains to be elucidated, as well as the molecular basis in which it relies.

Reactive synaptogenesis occurs following the partial loss of an afferent input, when the remaining terminals from the incomplete lesion sprout and occupy the vacant spaces left by the degenerating terminals (Lund and Lund 1971; Matthews et al. 1976; Lee et al. 1977; Mendell et al. 1978; Nadler et al. 1980b; Sedivec et al. 1983; Masliah et al. 1991; Bäurle et al. 1992; Zhang et al. 1995). Thus, in the long term, the physiological properties of reinnervated neurons might recover, or be modified, depending on the signals encoded by the reinnervating axons. In the case of medial rectus motoneurons, the long-term (2 months after lesion) recovery observed after ATD lesion could be explained by sprouting from the MLF projection. The transection of the MLF also produces some degree of (partial) recovery with time (Hernández et al. 2017a) and, therefore, sprouting from the ATD projection after MLF lesion, although likely less prominent, cannot be excluded.

In this work, we aim to evaluate the short-term events (24, 48, and 96 h post-lesion), at the presynaptic level, which take place early after partial deafferentation of medial rectus motoneurons to elucidate whether a sprouting process might support the long-term (2 months) physiological recovery described in deafferented medial rectus motoneurons (Hernández et al. 2017a). In this line, it is important to emphasize that neurotrophic factors, such as neurotrophins, have been described to increase in response to deafferentation (Johnson et al. 2000), and could play an important role in the reactive synaptogenesis process induced by lesion. Both inputs to medial rectus motoneurons (abducens internuclear and vestibular neurons) have been described to express the high-affinity receptors of neurotrophins, TrkA, TrkB and TrkC (Benítez-Temiño et al. 2004), which implies that they can respond to these neurotrophic molecules. Therefore, we have also investigated changes in neurotrophin content during the first 4 days after medial rectus motoneuron deafferentation, which could mediate the synaptic remodeling on these cells after the selective lesion of the ATD or the MLF.

Materials and methods

Male Wistar rats, weighing 250–300 g, were divided into 6 different groups to carry out the lesion of either the MLF (9 animals) or the ATD (9 animals), and sacrificed 24, 48 or 96 h after lesion (3 rats for each time point).

Selective deafferentation of medial rectus motoneurons

Under deep anesthesia (sodium pentobarbital, 35 mg/kg, i.p.), animals were placed in a stereotaxic frame. The skin and muscles above the skull were gently removed and a hole was drilled in the occipital bone. A custom-made blade was guided using a Camberra-type micromanipulator towards the appropriate coordinates (Paxinos and Watson 2009): 3.5 mm posterior to lambda, 7.5 mm deep, and using an anterior angle of 35°. For MLF section, the blade was 0.2 mm wide and its left corner was placed at the midline, to transect the right MLF unilaterally. For ATD section, a blade 0.5 mm wide was located 0.2 mm to the right of the midline, for transection of the right ATD. In this way, medial rectus motoneurons of the right oculomotor nucleus resulted partially deafferented of either the MLF or the ATD inputs (Fig. 1a). At the end of the surgical procedure, the skin was sutured and animals were monitored frequently for postsurgical care.

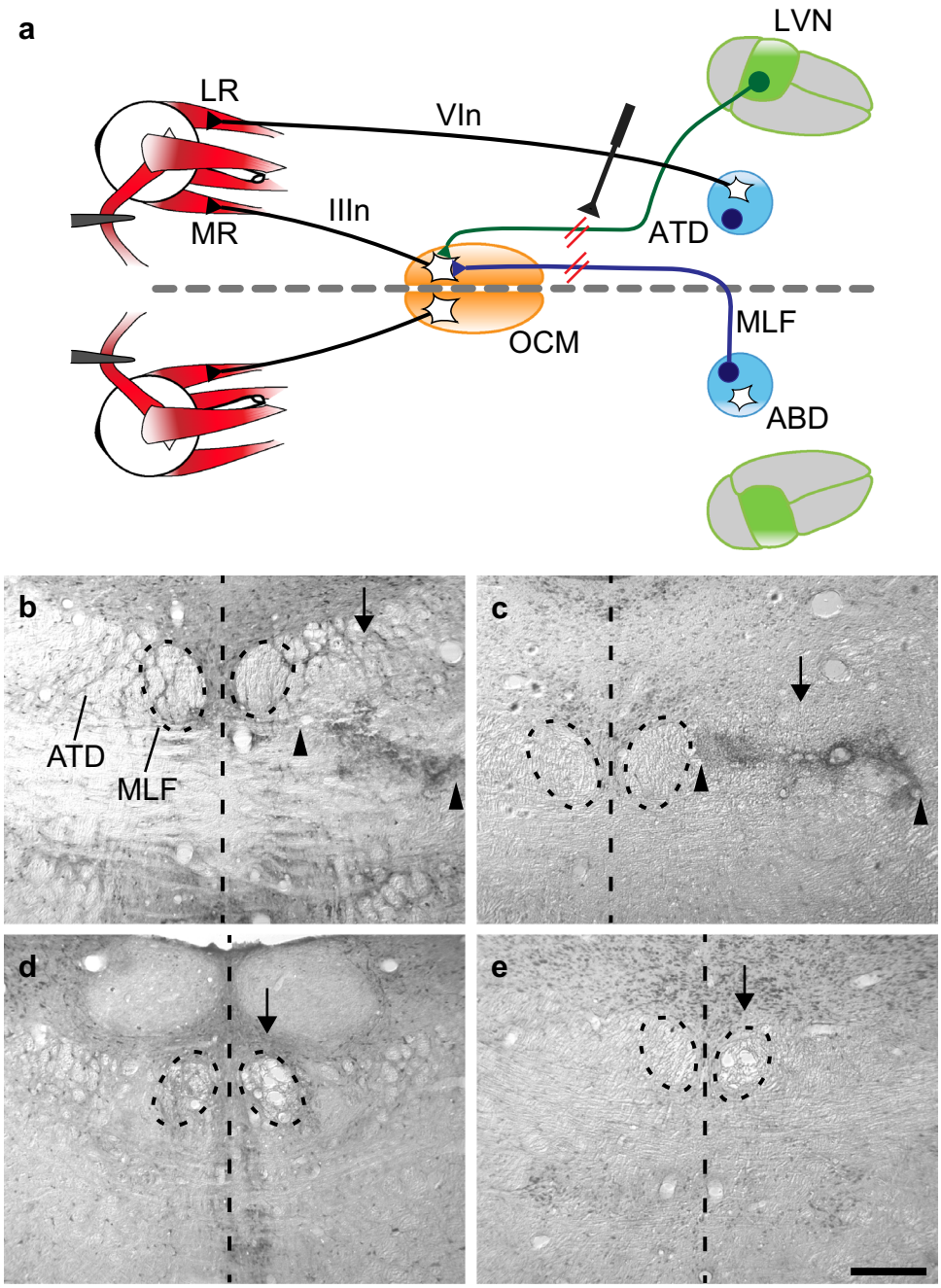

Fig. 1 Experimental design and lesion assessment. **a** Schematic diagram of a simplified oculomotor system in horizontal view, showing the main circuits implicated in conjugated horizontal gaze. Note that medial rectus (MR) motoneurons, which control horizontal eye movements, located in the oculomotor nucleus (OCM), receive two major inputs: one arising from the contralateral abducens (ABD) internuclear neurons whose axons course through the medial longitudinal fascicle (MLF), and the other originating in the ipsilateral lateral vestibular nucleus (LVN) and projecting through the ascending tract of Deiters (ATD). Lesions were made in either of these two projections to analyse the possible induction of compensatory mechanisms. Other abbreviations: *LR* lateral rectus muscle, *IIIn* third cranial nerve, *VIn* sixth cranial nerve. Lesion sites at the MLF or ATD are indicated by red lines. **b**, **c** Images showing coronal pontine sections at the lesion site after ATD transection, stained using either calretinin immunolabeling (**b**) or toluidine blue staining (**c**). Arrowheads point to the mediolateral ends of the lesion. Arrows point to the lesion side. Note that the lesion did not affect the MLF (encircled by dashed lines). Vertical dashed lines indicate midline. **d**, **e** Same as in **b**, **c**, but sections were obtained from a MLF-sectioned animal. Calibration bar: 300 µm

Retrograde medial rectus motoneuron labeling

Medial rectus muscles were injected with rhodamine isothiocyanate (Sigma, St. Louis, MO, USA) for motoneuron retrograde identification. Deeply anesthetized animals were restrained and medial rectus muscles were bilaterally injected with 1 µl of 20% rhodamine prepared in a solution of 2% dimethylsulfoxide, using a Hamilton syringe.

In the case of animals destined to the groups of 48 or 96 h, rhodamine injections and lesion were performed during the same surgical session. Since rhodamine requires a minimum period of 48 h to reach the motoneuron soma, animals of the 24 h group were anaesthetized and injected 24 h previous to lesion to guarantee the minimum transport period needed to allow rhodamine to reach the motoneuron soma. Thus, only this group of animals (24 h) underwent two surgeries.

Immunohistochemistry

Animals were deeply anesthetized (sodium pentobarbital, 50 mg/kg, i.p.), and perfused transcardially with 0.9% saline followed by 4% paraformaldehyde, prepared in phosphate buffer 0.1 M, pH 7.4. After cryoprotection in 30% sucrose prepared in phosphate buffered saline (PBS), the brainstem was dissected. Coronal sections, 40-µm-thick, were cut using a cryostat, and collected serially in a solution of glycerol-PBS (1:1) for storage at − 20 °C.

To assess the proper localization of the lesion site, brainstem sections from the mesopontine junction were selected. The proximal ends of sectioned axons were identified by immunocytochemistry against calretinin (goat anti-calretinin; AB1550; Chemicon, Temecula, CA, USA), a calcium-binding protein that is selectively expressed by both abducens internuclear neurons and neurons located at the ventral lateral vestibular nucleus (de la Cruz et al. 1998; Highstein and Holstein 2006). Sections were blocked with 10% normal donkey serum (NDS) in PBS with 0.1% Triton X-100 (PBS-T) for 45 min, and incubated at room temperature for 12 h in a solution containing the primary antibody (1:2500) in PBS-T with 0.05% sodium azide and 5% NDS. Sections were then rinsed in PBS-T and incubated for 2 h in the secondary antibody solution (biotinylated donkey anti-goat IgG, 1:250 in PBS-T; Vector Laboratories, Burlingame, CA, USA). After several washes, slices were incubated for 90 min in the avidin–biotin-HRP complex (ABC, Vector Laboratories) prepared in PBS-T. Following sequential washes in PBS, Tris–HCl buffered saline pH 7.4, Tris buffer 0.1 M pH 7.4 and Tris buffer 0.1 M pH 8, tissue was incubated in a solution of 0.05% 3,3′-diaminobenzidine tetrahydrochloride as the chromogen, 0.01% hydrogen peroxide and nickel sulphate 1 mM prepared in Tris buffer 0.1 M pH 8. Sections were thoroughly washed, mounted in glass slides and cover-slipped with DPX (Sigma). In addition, some sections were selected for Nissl counter-staining using toluidine blue. All animals included in this study presented the complete transection of either the MLF or the ATD.

For each animal, every fourth section was selected to characterize the synaptic organization at the medial rectus motoneuron subdivision of the oculomotor nucleus. Immunofluorescence directed against calretinin was used to evaluate MLF or ATD innervation. After several washes and blockade, slices were incubated overnight at room temperature in a solution containing the primary antibody (goat anti-calretinin, 1:500), prepared as mentioned above. Sections were then rinsed and incubated for 2 h in the secondary antibody solution (donkey anti-goat IgG coupled to Cy5, 1:200; Jackson Immunoresearch, West Grove, PA, USA), prepared in PBS-T. After several washes in PBS, sections were mounted on glass slides and cover-slipped using Dako as the mounting medium (DakoCytomation, Glostrup, Denmark).

Besides calretinin immunostaining, the remaining three series were used to check possible changes in neurotrophin expression in partially deafferented medial rectus motoneurons. For this purpose, we performed immunocytochemistry against brain-derived neurotrophic factor (BDNF), neurotrophin-3 (NT-3) or nerve growth factor (NGF). Sections were incubated for 10 min in PBS with 1% sodium borohydride for antigen retrieval, blocked as described above, and incubated overnight at room temperature in a solution containing the primary antibody in PBS-T with 0.05% sodium azide and 5% NDS (rabbit anti-BDNF sc-546, rabbit anti-NT-3 sc-547 or rabbit anti-NGF sc-548, 1:100; Santa Cruz Biotechnology, Dallas, TX, USA). Sections were then rinsed in PBS-T and incubated in the secondary antibody (biotinylated donkey anti-rabbit 1:250, Vector Laboratories) for 2 h. After several washes, slices were immersed in a solution containing streptavidin conjugated with Cy2 (1:800 in PBS, 45 min; Jackson ImmunoResearch). Finally, sections were thoroughly washed in PBS, mounted in glass slides and cover-slipped using Dako.

Image analysis

Sections were visualized using a Zeiss LSM Duo confocal microscope (Zeiss, Oberkochen, Germany). Lasers DPSS 561 nm, argon 488 nm and HeNe 633 nm were used to excite rhodamine, Cy2, and Cy5, respectively.

Two different kinds of analyses were carried out to evaluate the time course of afferent reorganization. First, the synaptic coverage around the somata of medial rectus motoneurons was measured bilaterally for control-experimental comparisons. For this purpose, *z*-stack images at 63× magnification were captured. Neurons with visible nucleus were selected for the analysis using ImageJ software (NIH).

The somatic perimeter of medial rectus motoneurons was measured in all experimental situations to check possible changes in soma size. Somatic synaptic coverage was calculated as the percentage of the soma perimeter that was covered by calretinin-immunoreactive boutons, and expressed as calretinin linear density. We also measured the number of calretinin-immunoreactive terminals per 100 µm of soma perimeter. Second, the synaptic density of calretinin-immunopositive boutons in the neuropil (the area surrounding medial rectus motoneuron cell bodies) was calculated from 3 × 3-stitched images, at 40× magnification. Random-selected squares of approximately 20 × 20 µm through the neuropil were used to measure the intensity of calretinin immunostaining (i.e., optical density) at the medial rectus subdivision of the oculomotor nucleus. Mean background level, obtained from four different squares selected from non-stained areas, was subtracted, and the values of optical density were normalized with respect to the control side of the same section.

To evaluate the presence of BDNF and NT-3 in medial rectus motoneurons, optical density was measured inside the cytoplasm of control and deafferented cells of the same section. After background level subtraction, data were expressed for each cell as the percentage with respect to the mean of the control values in the same section. NGF was not present inside motoneuron somata, but stained dendritic-like processes in the neuropil, as previously described (Hernández et al. 2017b). Thus, we compared the presence of NGF under the different experimental conditions by measuring optical density in the neuropil as explained above. Data were expressed as mean ± SEM. Comparisons between control, MLF- or ATD-sectioned animals, at different post-lesion time intervals, were performed using the two-way ANOVA test, with an overall level of significance of 0.05, followed by post hoc comparisons using the Holm–Sidak method for multiple comparisons. Statistics was performed by means of SigmaPlot software, version 11.0 (Systat Software, Inc., San Jose, CA, USA).

Results

Lesions of the MLF or the ATD were assessed in coronal sections at the mesopontine junction that were treated for immunocytochemistry against calretinin (Fig. 1b, d) or Nissl staining (Fig. 1c, e).

Time course of changes in synaptic coverage on medial rectus motoneurons after partial deafferentation

Both abducens internuclear and vestibular neurons projecting to medial rectus motoneurons express calretinin (de la Cruz et al. 1998; Hernández et al. 2017a). Thus, we used calretinin as a marker to selectively label and compare the extension of afferent terminals arising from each of these two projections around medial rectus motoneurons, after either MLF or ATD transection.

First, we analyzed the optical density of calretinin-immunostained sections through the medial rectus subdivision of the oculomotor nucleus after each type of lesion, to compare the extension of the remaining (intact, unlesioned) projection in the neuropil at different time points. Data were normalized with respect to the control side (Fig. 2g, control).

Partial deafferentation induced by ATD lesion produced a decrease in calretinin staining (two-way ANOVA, $F_{(4,3627)}$=21.03, Holm–Sidak method for pairwise multiple comparisons, $p < 0.001$) that was evident 24 h after lesion (79.84 ± 3.17%, n =180, $p < 0.001$; Fig. 2a, h), and even more pronounced by 48 h post-lesion (64.49 ± 4.14%, n = 234, $p < 0.001$; Fig. 2b, h). However, 96 h after ATD lesion there was a rise in calretinin staining (90.39 ± 2.86%, n = 324, $p < 0.001$; Fig. 2c, h). Although this increase was lower than the control value ($p < 0.001$), it was higher than mean values obtained at shorter time points ($p = 0.012$ and $p < 0.001$ when compared with 24 and 48 h, respectively; Fig. 2h, green columns). These data could be interpreted as the result of the formation of new terminals after ATD transection, probably originating from the remaining calretinin-positive afferents, i.e., the abducens internuclear axons.

24 and 48 h after MLF transection, results were similar to those obtained in ATD-lesioned animals at the same time points, that is, a significant decrease in calretinin optical density (24 h: 80.83 ± 1.81%, n = 369, Fig. 2d, h; 48 h: 62.16 ± 1.36%, n = 304, Fig. 2e, h). Surprisingly, in contrast to ATD lesion, mean optical density did not recover 96 h after the lesion of the MLF. Instead, it remained similar to that observed 24 h before, and lower to control or values obtained 96 h after ATD transection (59.76 ± 1.57%, n = 400, $p < 0.001$; Fig. 2f, h, blue columns). Thus, in the case of MLF lesion, we could not identify any compensatory sprouting mechanism carried out by the remaining intact afferent system, i.e., the ATD projection.

We also compared the percentage of the soma perimeter that was occupied by calretinin-immunoreactive boutons, after either MLF or ATD transection. As described in the neuropil, ATD transection produced a progressive reduction in synaptic innervation around medial rectus motoneuron somata when compared to control (Fig. 3a, c, g, h). However, this tendency was reversed at 96 h post-lesion, when there was an increase in somatic synaptic coverage (Fig. 3e). MLF transection also produced a progressive decrease in the somatic innervation of medial rectus motoneurons, although, opposite to ATD results, this trend was present at any time point (Fig. 3b, d, f).

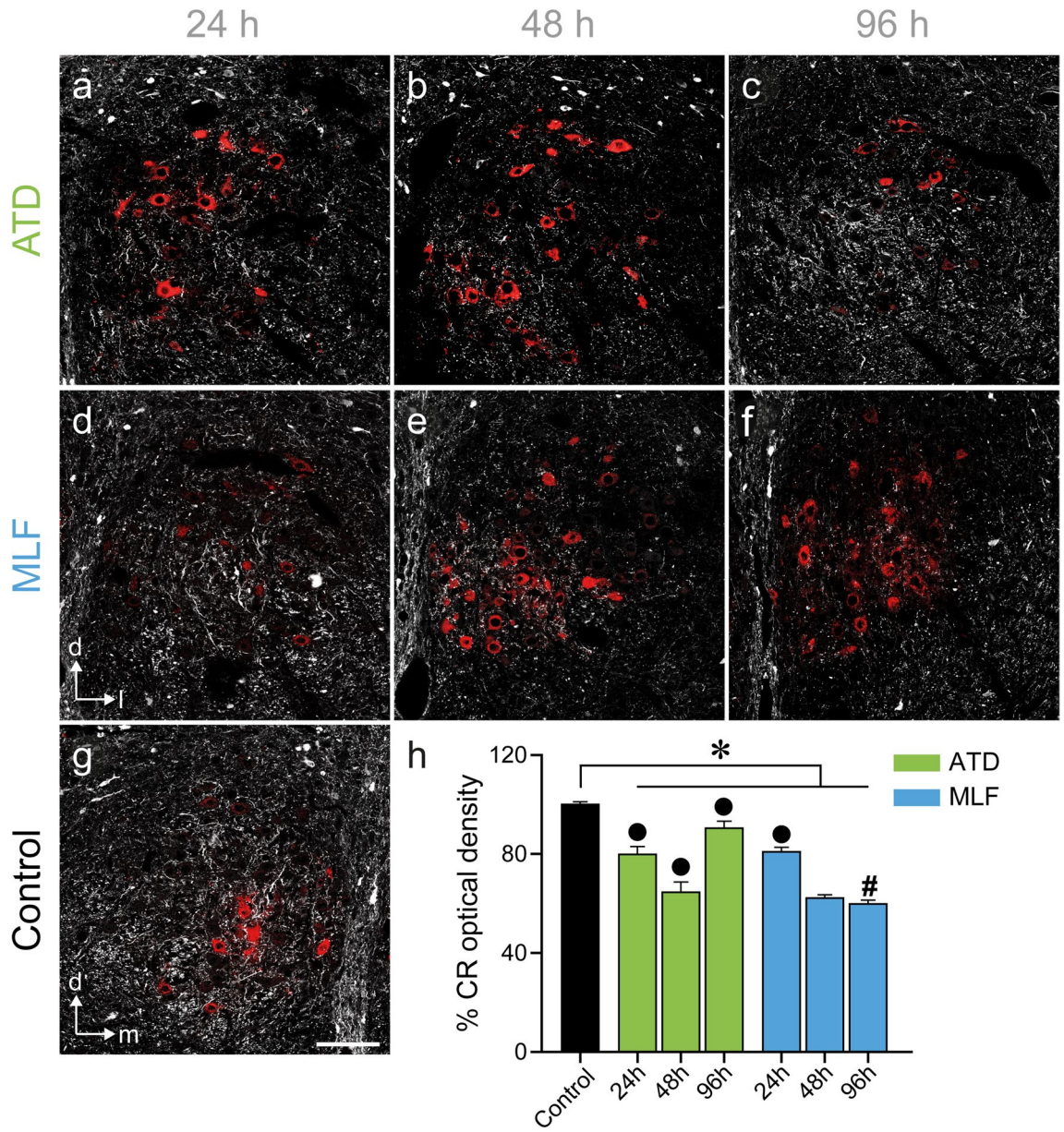

Fig. 2 Time course of changes in calretinin immunostaining in the neuropil surrounding medial rectus motoneurons. **a**–**g** Confocal microscopy images of the medial rectus motoneuron subgroup of the oculomotor nucleus, 24 (**a**, **d**), 48 (**b**, **e**) or 96 h (**c**, **f**) after ATD (**a**–**c**) or MLF (**d**–**f**) transection, and in the control situation (**g**). Medial rectus motoneurons were identified by retrogradely transported rhodamine (red). Calretinin immunostaining is shown in white. Calibration bar: 100 µm. **h** Bar plot showing mean ± SEM of calretinin (CR) immunostaining intensity (measured as optical density) in the control group and at every time point analyzed for both types of lesion and expressed normalized to the control side. Asterisk indicates differences with respect to control, dots represent differences with respect to other time points within the same lesion type, and hashtags point to differences between lesions within the same time point. Two-way ANOVA test followed by Holm–Sidak method for multiple pairwise comparisons ($p < 0.001$). $n = 1820$ (control), 180, 234, 324 (ATD lesion 24, 48 and 96 h after lesion, respectively) and 369, 304, 400 (MLF lesion 24, 48 and 96 h after lesion, respectively). Labels in **d** for **a**–**f**: *l* lateral and *d* dorsal. Labels in **g** for **g**: *m* medial, *d* dorsal

Quantitatively, we did not observe any change in the somatic perimeter of medial rectus motoneurons at any time point after ATD or MLF transection (87.32 ± 0.79 µm for control cells, $n = 315$; Fig. 3i). However, there were changes in the percentage of soma perimeter covered by calretinin-positive terminals after both types of lesion (linear density; two-way ANOVA, $F_{(4841)} = 39.26$; Holm–Sidak method for pairwise multiple comparisons, $p < 0.001$).

The linear density (measured as the percentage of the somatic perimeter surrounded by calretinin-immunoreactive

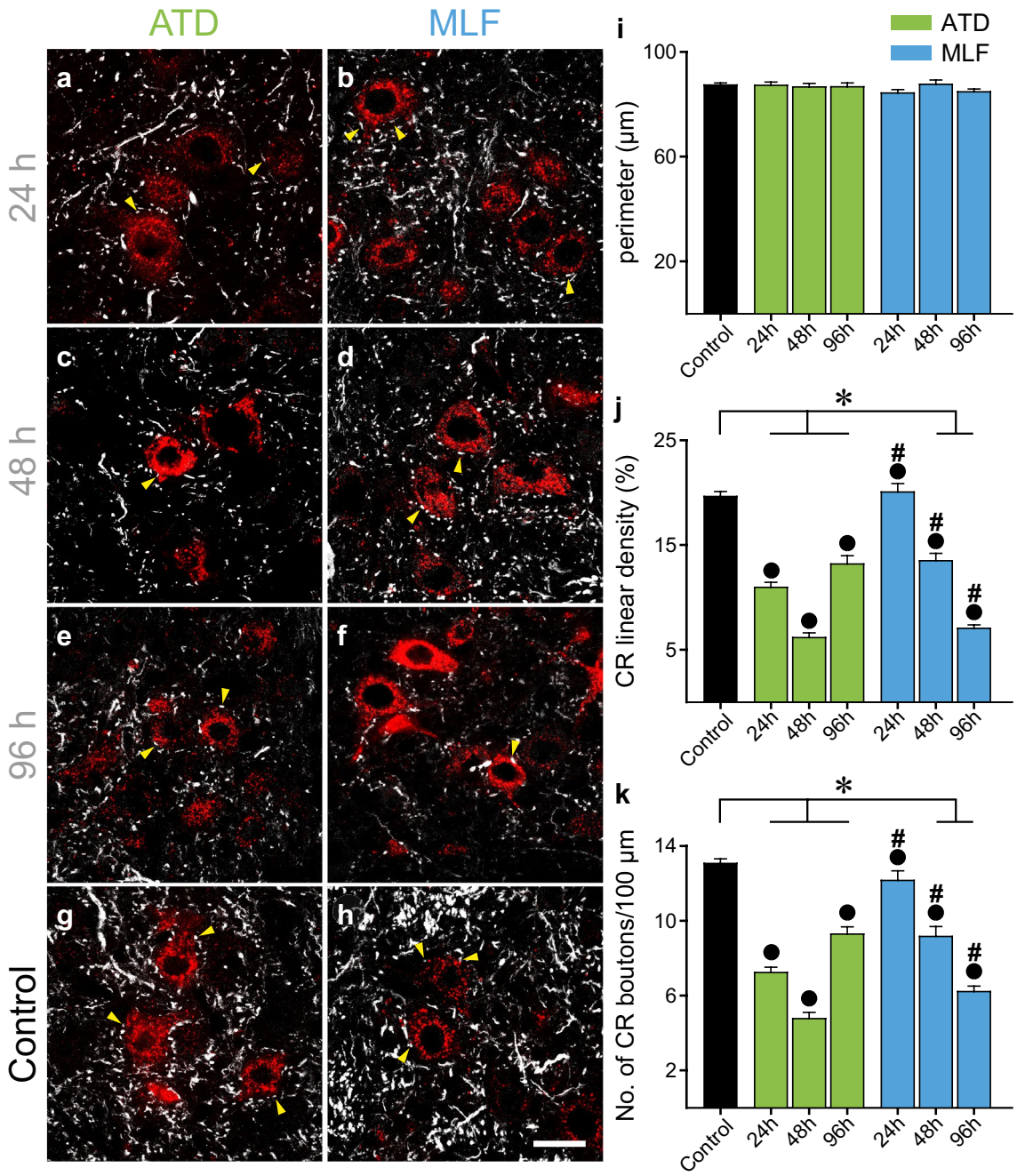

Fig. 3 Changes in synaptic coverage around medial rectus motoneuron somata after selective deafferentation. **a**–**h** Confocal microscope images showing rhodamine-stained medial rectus motoneurons 24 (**a**, **b**), 48 (**c**, **d**) or 96 h (**e**, **f**) after ATD (left column) or MLF (right column) transection, and in the control situation (**g**, **h**). Axons and terminal ramifications belonging to abducens internuclear neurons (left column, ATD lesion) or vestibular nucleus (right column, MLF lesion) were immunostained against calretinin (in white). Arrowheads point to examples of terminals that were counted Calibration bar: 25 µm. **i**–**k** Histograms comparing several morphological parameters between the control situation (black bar), and data obtained 24, 48 and 96 h after ATD (green bars) or MLF (blue bars) transection. Data correspond to mean ± SEM. **i** Bar chart comparing mean medial rectus motoneuronal soma perimeter in the control situation and 24, 48 and 96 h after partial deafferentation. No statistical differences were found. **j** Synaptic coverage measured as the percentage of the soma perimeter covered by calretinin (CR)-immunostained synaptic terminals. **k** Synaptic coverage measured as the number of boutons per 100 µm of somatic perimeter. Asterisks indicate differences with the control group, dots represent differences with respect to other time points within the same lesion type, and hashtags point to differences between lesions within the same time point. For **i**–**k**, two-way ANOVA test followed by Holm–Sidak method for multiple pairwise comparisons ($p < 0.001$ for **j** and **k**). Levels of significance for pairwise comparisons are indicated in the text; $n = 315$ (control), 95, 80, 78 (ATD-depleted cells 24, 48 and 96 h after lesion, respectively) and 98, 71, 108 (MLF-depleted cells 24, 48 and 96 h after lesion, respectively)

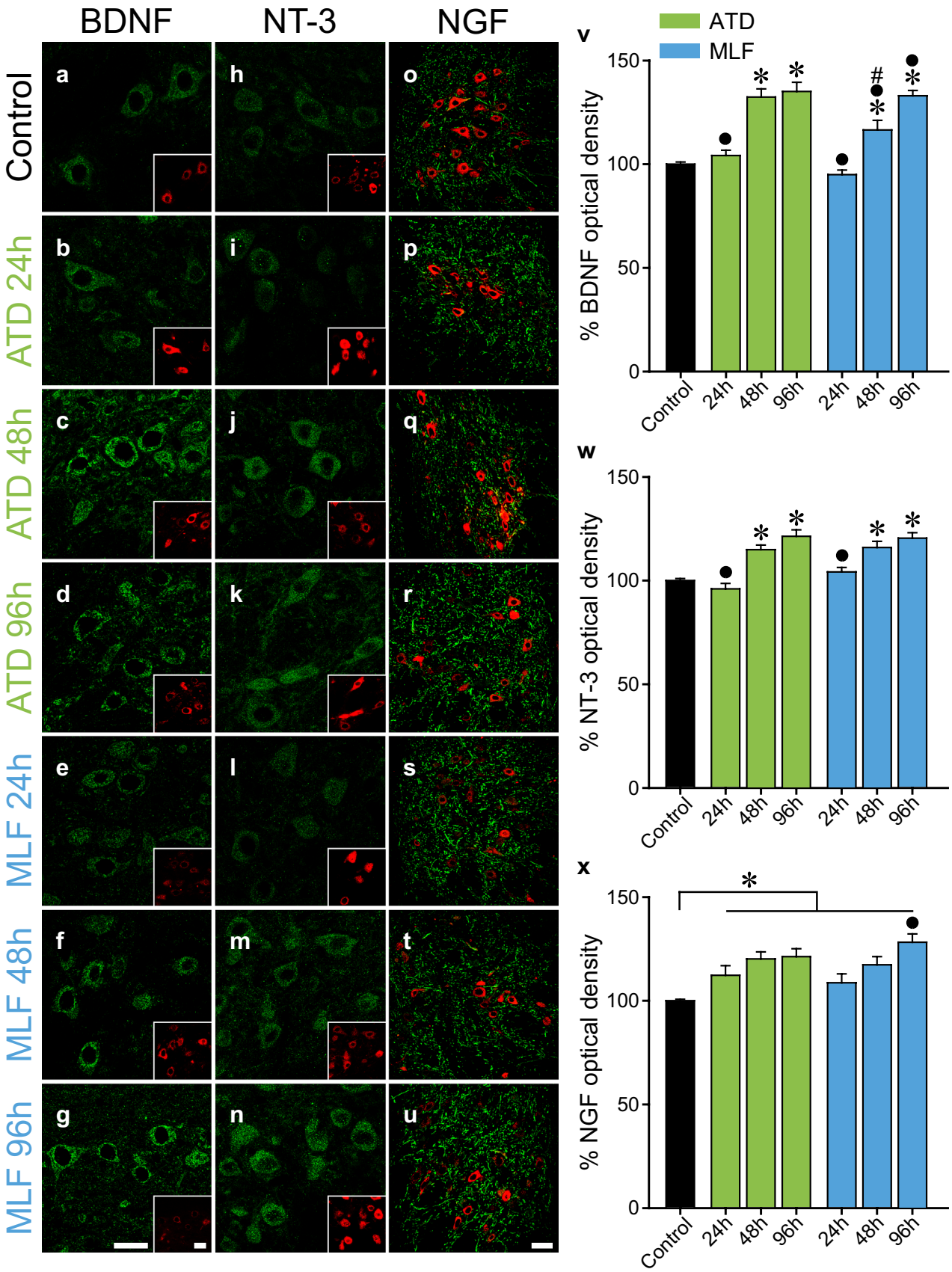
BDNF
NT-3
NGF
Control
ATD 24h
ATD 48h
ATD 96h
MLF 24h
MLF 48h
MLF 96h
a
b
c
d
e
f
g
h
i
j
k
l
m
n
o
p
q
r
s
t
u
v
ATD
MLF
% BDNF optical density
150
100
50
0
Control
24h
48h
96h
24h
48h
96h
w
% NT-3 optical density
x
% NGF optical density

◂**Fig. 4** Time course of changes in neurotrophin content in medial rectus motoneuron cell bodies after partial deafferentation. **a**–**u** Confocal microscope images showing BDNF (**a**–**g**), NT-3 (**h**–**n**) or NGF (**o**–**u**) immunostaining in rhodamine-identified (insets) medial rectus motoneurons in the control situation (**a**, **h**, **o**), 24 (**b**, **i**, **p**), 48 (**c**, **j**, **q**) or 96 h (**d**, **k**, **r**) after ATD transection, or 24 (**e**, **l**, **s**), 48 (**f**, **m**, **t**) or 96 (**g**, **n**, **u**) hours after MLF transection. Calibration bars: 25 µm in **g** for **a**–**n**, and in **u** for **o**–**u;** 30 µm in insets (in **g**). Bar plots comparing BDNF (**v**), NT-3 (**w**) or NGF (**x**) immunostaining intensity (measured as optical density) inside medial rectus motoneurons in control animals (black bars), after ATD transection (green bars) or MLF transection (blue bars) at different time points. Data correspond to mean ± SEM and are expressed as percentages relative to the control side. **v**. Number of motoneurons analyzed: $n = 769$ (control), 135, 90, 92 (ATD-depleted cells 24, 48 and 96 h after lesion, respectively) and 150, 91, 236 (MLF-depleted cells 24, 48 and 96 h after lesion, respectively). **w** Number of motoneurons analyzed: $n = 683$ (control), 92, 159, 100 (ATD-depleted cells 24, 48 and 96 h after lesion, respectively) and 117, 108, 155 (MLF-depleted cells 24, 48 and 96 h after lesion, respectively). **x** Number of motoneurons analyzed: $n = 3300$ (control), 150, 200, 200 (ATD-depleted cells 24, 48 and 96 h after lesion, respectively) and 175, 175, 200 (MLF-depleted cells 24, 48 and 96 h after lesion, respectively). Significance levels for pairwise comparisons indicated in the text. Asterisks indicate differences with the control group, dots represent differences with respect to other time points within the same lesion type, and hashtags point to differences between lesions within the same time point. For **v**–**x**, two-way ANOVA test followed by Holm–Sidak method for multiple pairwise comparisons, $p < 0.001$ for **v**, **w** and **x**

boutons) decreased after ATD transection with respect to control (19.63 ± 0.47%, $n = 315$ for control; 10.95 ± 0.76%, 6.16 ± 0.44% and 13.19 ± 0.78%, at 24, 48 and 96 h post-lesion, $n = 95$, 80 and 78, respectively, $p < 0.001$; Fig. 3j, green columns). However, there was a partial recovery 96 h after ATD lesion, which did not reach control values, but was statistically higher than the calretinin linear density obtained in previous time points ($p = 0.049$ and $p < 0.001$ when compared with 24 and 48 h, respectively).

The decrease in calretinin-immunoreactive synaptic coverage (i.e., linear density) after MLF transection was slower than after ATD lesion ($p < 0.001$). Thus, 24 h after MLF lesion mean values were similar to controls (20.05 ± 0.80%, $n = 98$). However, in the following time points, the tendency to the reduction in linear density was constant (13.50 ± 0.70% and 7.05 ± 0.32%, $n = 71$ and 108, for 48 and 96 h post-lesion, respectively, $p < 0.001$; Fig. 3j, blue columns). The reduction was more severe in ATD- than in MLF-lesioned animals at any time point ($p < 0.001$), except for the 96 h group, when, as described above, there was a recovery in synaptic coverage after ATD section with respect to 48 h, which was not present in MLF-lesioned animals. These results could indicate that the degenerative process of axonic terminals that takes place in response to MLF transection was still present 96 h post-lesion, but in the case of ATD-lesioned animals, a compensatory synaptic mechanism would contribute to the formation of new calretinin-positive terminals from the (intact) MLF projection that would compensate quantitatively for the disappearance of disconnected terminals.

In accordance to linear density changes, we found a similar time course of changes in the number of boutons per 100 µm of soma perimeter (two-way ANOVA, $F_{(4841)} = 32.53$; Holm–Sidak method for pairwise multiple comparisons, $p < 0.001$; Fig. 3k, same sample of cells at each time point after ATD or MLF lesion as in Fig. 3j). Control motoneurons were covered by a mean value of 13.06 ± 0.25 boutons/100 µm of perimeter. 24 h post-lesion, this value was reduced in ATD-lesioned animals (7.24 ± 0.28 boutons/100 µm; $p < 0.001$), but not in MLF-lesioned animals (12.15 ± 0.51 boutons/100 µm). 48 h post-lesion, after both ATD or MLF transection there was a decrease in the number of boutons located around the cell bodies of medial rectus motoneurons (4.77 ± 0.33 and 9.16 ± 0.53 boutons/100 µm, respectively) when compared with both control and 24 h post-lesion ($p < 0.001$), although the effect was more drastic after the transection of the ATD ($p < 0.001$). However, at 96 h there was a rise in the number of boutons after ATD transection, which was not present after MLF lesion (Fig. 3k, 96 h). Rather, the number of boutons after MLF transection was even lower at 96 h (9.29 ± 0.38 and 6.21 ± 0.29 boutons/100 µm, after ATD or MLF lesion, respectively; $p < 0.001$).

Time course of changes in neurotrophin content in medial rectus motoneurons after partial deafferentation

BDNF and NT-3 were present in the soma of the great majority of control medial rectus motoneurons (97.45 ± 1.17% and 96.82 ± 1.64%, respectively), as we have described previously (Hernández et al. 2017a, b). Partial deafferentation did not change these percentages at any time point (two-way ANOVA).

The presence of BDNF or NT-3 in medial rectus motoneurons in the different situations was measured as the percentage of somatic optical density with respect to the mean obtained in the control side. We found an increase in BDNF content inside the cytoplasm of partially denervated motoneurons from 48 h post-lesion onwards (two-way ANOVA, $F_{(4,1559)} = 22.55$, Holm–Sidak method for pairwise multiple comparisons, $p < 0.001$; Fig. 4a–g, v). Thus, in the case of ATD-lesioned animals and 24 h post-lesion, the content of BDNF was similar to control values (104.20 ± 2.50%, $n = 135$). However, 48 and 96 h post-lesion, mean optical density increased to 132.39 ± 3.93% ($n = 90$) and 135.07 ± 4.46% ($n = 92$), respectively ($p < 0.001$; Fig. 4v, green columns). Similarly, 24 h after MLF transection we found no change in BDNF optical density (94.98% ± 2.23, $n = 150$) when compared to control values ($n = 769$), although from that point onwards,

optical density increased progressively (116.50 ± 4.65%, $n = 91$ and 132 ± 2.59%, $n = 236$, for 48 and 96 h post-lesion, respectively, $p < 0.001$; Fig. 4v, blue columns). 96 h post-lesion the intensity of the staining was similar in both experimental groups, so the transection of either the MLF or the ATD produced the same final effect on BDNF expression in partially deafferented medial rectus motoneurons.

In line with the BDNF results, NT-3 immunocytochemistry produced, 24 h after the lesion of the ATD or the MLF, a staining that was similar to control values ($n = 683$), but increased 48 and 96 h after the injury of either of the two tracts (two-way ANOVA, $F_{(4,1410)} = 8.76$; Holm–Sidak method for pairwise multiple comparisons, $p < 0.001$; Fig. 4h–n, w). Quantitatively, optical density 24 h after ATD or MLF transection was 95.96 ± 2.68% ($n = 92$) and 104.19 ± 2.13% ($n = 117$) of control values, respectively (Fig. 4w). 48 h after partial deafferentation, these values increased to 114.91 ± 2.20% ($n = 159$) and 115.95 ± 2.94% ($n = 108$), respectively, in comparison to control values, which were significantly higher than both control and 24 h values ($p < 0.001$), and remained high at 96 h post-lesion (121.33 ± 3.17%, $n = 100$ and 120.44 ± 2.66%, $n = 155$, respectively; $p < 0.001$).

Opposite to BDNF and NT-3 staining, but in line with our previous results (Hernández et al. 2017b), NGF immunocytochemistry barely stained medial rectus motoneuron somata. Instead, a profuse neuropil staining was present, frequently associated to long filamentous processes (Fig. 4o–u). This pattern of staining was constant for all control and experimental groups. However, the intensity of the staining, measured as the percentage of optical density mean values with respect to control, varied with time (two-way ANOVA, $F_{(4,4396)} = 4.53$; Holm–Sidak method for pairwise multiple comparison, $p < 0.001$; Fig. 4x). As early as 24 h after either ATD or MLF transection, optical density rose significantly to 112.25 ± 4.65% ($n = 150$; $p < 0.001$) and 108.66 ± 4.27% ($n = 175$; $p = 0.015$), respectively, with respect to control values ($n = 3300$). Mean values remained similar 48 and 96 h after ATD transection (120.18 ± 3.39%, $n = 200$ and 121.29 ± 3.79%; $n = 200$, respectively) with respect to 24 h data, and elevated with respect to control ($p < 0.001$). Finally, 48 h after MLF transection, NGF staining was significantly stronger than in controls (117.36 ± 3.91%, $n = 175$, $p < 0.001$), and rose to 128.19 ± 4.04% ($n = 200$, $p < 0.001$) 96 h post-lesion. Thus, in summary, the intensity of immunostaining against BDNF and NT-3 increased from 48 h post-lesion and was maintained at high values by 96 h. NGF immunostaining intensity increased from the earliest time point analyzed (24 h) and continued high at 48 and 96 h.

Discussion

The present study compares the different plastic changes of the two main projections that mediate conjugate horizontal eye movements, and their ability to compensate for each other after selective input depletion on medial rectus motoneurons. Thus, we performed the axotomy of either abducens internuclear neurons or lateral vestibular neurons to induce medial rectus motoneuron partial, selective deafferentation. We have previously shown that partial deafferentation in the oculomotor system of cats produces a recovery of function (i.e., in eye movements and motoneuronal discharge activity), which is already perceptible 5 days after lesion. Thus, we investigated the plastic mechanisms underlying this recovery in the short term, which is during the first 4 days after lesion. In spite of the similar increase in neurotrophin content in/around affected motoneurons, results differed depending on the type of lesion. Thus, vestibular deafferentation produced a rapid decrease in synaptic coverage that, however, improved 96 h after lesion. This recovery could be related to a previous rise in neurotrophin content. On the contrary, abducens input depletion produced synaptic terminal degeneration, which lasted the whole experimental period analyzed, without any sign of recovery.

These results point to plastic mechanisms performed by the abducens internuclear neuron inputs to refill the synaptic vacant spaces left on medial rectus motoneurons after ATD lesion. However, MLF transection did not induce a similar response in, otherwise intact, vestibular inputs. This difference probably implies a higher plastic capability of the abducens internuclear neuron pathway when compared with that of vestibular neurons connecting to medial rectus motoneurons.

Synaptic organization of medial rectus motoneuron afferents

24 h after lesion, the effects on synaptic coverage around medial rectus motoneuron cell bodies were more drastic after vestibular lesion than after the axotomy of abducens internuclear neurons. On the contrary, neuropil analyses at this time point revealed a similar reduction after both types of lesion. These differences could reflect a distinct anatomical distribution of the two main inputs on medial rectus motoneurons, as described previously (Nguyen et al. 1999; Hernández et al. 2017a). Thus, vestibular afferents would terminate preferentially on motoneuron somata, while axons from the abducens nucleus would end preferentially on dendrites. Differences in the degradation rate of disconnected terminals cannot be discarded. Indeed,

the velocity of Wallerian degeneration, synapse disorganization and presynaptic terminal removal vary between groups of neurons (State and Dessouky 1977; Cotman et al. 1981).

Increase in medial rectus motoneuron innervation after vestibular lesion

Despite the rapid decrease in calretinin-positive terminals around medial rectus motoneurons after ATD transection, 96 h after lesion there was an increase both in the synaptic coverage around somatic perimeter and in the density of terminals in the neuropil. Given the immunoreactivity of these new terminals against calretinin, it might be concluded that their origin would be the abducens internuclear neuron population. The same process of compensatory sprouting after partial deafferentation has already been described in the hippocampus (Matthews et al. 1976; Lee et al. 1977; Masliah et al. 1991), visual (Lund and Lund 1971) and vestibular systems (Bäurle et al. 1992) and the spinal cord of mammals (Zhang et al. 1995). The present results would agree with those obtained previously in the cat, where the same type of lesion produced alterations in motoneuronal discharge pattern and in eye movements, which returned to normality between 3 and 5 days after lesion (Hernández et al. 2017a), and with similar approaches performed in different systems such as presynaptic sympathetic neurons in the spinal cord (Krassioukov and Weaver 1996). Thus, during the 3 days following lesion, a compensatory mechanism likely took place involving the activation of the molecular machinery needed for the extension of new axonal branches and the formation of new terminal boutons. The establishment of new synapses would lead to the recovery of the physiological properties of medial rectus motoneurons (Hernández et al. 2017a).

We have not analyzed possible synaptic remodeling carried out by other putative inputs. Medial rectus motoneurons receive inputs not only from second-order vestibular and abducens internuclear neurons, but also from GABAergic terminals whose origin remains to be clarified (de la Cruz et al. 1992). However, other authors have postulated that reactive synaptogenesis is carried out by axons with biochemical characteristics that resemble those of the original projection (Grinnell and Rheuben 1979; Cotman et al. 1981). According to this hypothesis, GABAergic neurons would not be a good candidate to replace the vacant spaces left after partial deafferentation. However, both abducens internuclear and lateral vestibular neurons are glutamatergic, so both projections would be good candidates to replace each other (Nguyen and Spencer 1999). It has also been postulated that synaptic replacement would be carried out preferentially by the enlargement of a preexisting afferent projection (Nadler et al. 1980a; Tessler et al. 1980; Cotman et al. 1981). Accordingly, it is unlikely that afferents to other extraocular motoneurons in the oculomotor nucleus, or even axons that course through the MLF different from those of the abducens internuclear neurons, could establish a new pathway onto medial rectus motoneurons.

In contrast to the lesion of the vestibular input (ATD), MLF transection had permanent effects on the synaptic organization around medial rectus motoneurons. In this case, ATD axons did not seem to have the same ability to sprout in response to the selective deafferentation of their target motoneurons. Differences in the ability to sprout and form new synapses onto partially deafferented neurons have also been described in the hippocampus (Cotman and Nadler 1978). Alternatively, or in addition, given the small size of the ATD projection on medial rectus motoneurons, which contains a much lower number of calretinin-immunopositive axons than those in the MLF (Hernández et al. 2017a), a hypothetical sprout of vestibular axons might not be sufficient to compensate the large loss of synaptic inputs arriving through the MLF. In other words, it could be a matter of insufficient compensation rather than the lack of a sprouting response. In fact, results obtained 96 h post-lesion could be misleading, since, in the case of ATD lesion, the boutons observed could reflect the coexistence of two opposing processes: the degeneration of those axons, which have been disconnected from their soma, and the formation of new terminals. Thus, the compensatory mechanism could be even larger than that revealed by the data. In the same line of argumentation, results from MLF-lesioned animals could also reflect the sum of still disappearing terminals (in fact, there is a reduction in synaptic coverage between 48 and 96 h) and newly formed terminals, which, however, would not be enough to compensate synapse degradation.

Role of neurotrophins in reactive synaptogenesis

The role of neurotrophins in reactive synaptogenesis after partial deafferentation was proposed decades ago (Cotman and Nieto-Sampedro 1984). Indeed, partial deafferentation leads to an increase in BDNF and NT-3 expression in motoneurons (Johnson et al. 2000) and cortical neurons (Endo et al. 2007). This newly formed neurotrophin pool may stimulate neurite growth (Ruit and Snider 1991; Cohen-Cory and Fraser 1995; Inoue and Sanes 1997), as well as the formation of new synapses (Nja and Purves 1978; Endo et al. 2007). In fact, axon sprouting after partial deafferentation in the spinal cord can be stimulated by exogenous neurotrophin supply (Jakeman et al. 1998; Scott et al. 2005), and the role of endogenous neurotrophins in the formation of new collateral axon branches has already been demonstrated (Gallo and Letourneau 1998; Atwal et al. 2000). Moreover, experiments of partial deafferentation in the pelvic ganglia have shown not only a synaptic remodeling with the formation of new synapses, but also an increase in TrkA expression

in those neurons generating new presynaptic terminals, which, therefore, would be more responsive to NGF (Keast and Kepper 2001).

In contrast to our results in the oculomotor system, deafferentation may produce a reduction in BDNF mRNA in spinal motoneurons (Gomez-Pinilla et al. 2004). This opposite response to the removal of afferents could be due to intrinsic differences between spinal and extraocular motoneurons. Thus, an important neurotrophic difference is that adult spinal motoneurons do not express the high-affinity NGF receptor TrkA (Lindsay 1994; Ferri et al. 2002), while extraocular motoneurons do (Benítez-Temiño et al. 2004; Morcuende et al. 2011). Also, exogenous NGF rescues these motoneurons from lesion-induced morphological and electrophysiological changes (Davis-López de Carrizosa et al. 2010), and the dependence of extraocular motoneurons on NGF, BDNF and NT-3 for survival during development (Morcuende et al. 2013), as well as for the maintenance of proper adult characteristics after lesion is well documented (Davis-López de Carrizosa et al. 2009, 2010). Altogether, it is likely that medial rectus motoneurons would not be only responsive to the delivery of neurotrophins, but that they would also regulate the availability of neurotrophins, which in turn influences the maintenance of their afferent inputs, thus acting as a retrograde source of neurotrophins.

Axonal sprouting stimulation could be mediated by the well-known growth-associated protein GAP-43, which is upregulated by neurotrophins (Perrone-Bizzozero et al. 1991, 1993; Mohiuddin et al. 1995; Federoff et al. 1988; Dinocourt et al. 2006; Geremia et al. 2010; Sanna et al. 2017). Accordingly, and considering that, first, the content in neurotrophins in medial rectus motoneurons increased after partial deafferentation, second, both abducens internuclear and lateral vestibular neurons express neurotrophin receptors (Benítez-Temiño et al. 2004), and third, the time course of changes in neurotrophin content preceded that of the partial recovery of calretinin-immunopositive terminals, it could be possible that, also in the oculomotor system, neurotrophins released by motoneurons in response to partial deafferentation would favor axonal sprouting from the remaining afferent system.

Our results showed a similar increase in neurotrophin content when comparing the effects of sectioning either the MLF or the ATD. However, the extent of synapse remodeling differed between the two types of lesion, so that abducens internuclear neurons seemed to be much more plastic than vestibular cells in terms of axon terminal sprouting. These differences could be explained considering several aspects. First, as stated above, the abducens projection to medial rectus motoneurons is much larger than the vestibular one (Hernández et al. 2017a). Thus, the selective removal of the vestibular input could easily be compensated by the abducens internuclear neuron sprouting. On the contrary, the removal of the abducens projection would be too massive to be relieved by sprouting of the (otherwise scarce) vestibular afferents. Second, MLF and ATD axons could respond with different sensitivity to the neurotrophins released by motoneurons. As stated above, both abducens internuclear neurons and lateral vestibular nucleus neurons express Trk receptors (Benítez-Temiño et al. 2004; Morcuende et al. 2011), but a quantitative analysis comparing the expression of these receptors in both populations is lacking. Finally, possible changes in Trk expression or localization after partial deafferentation of the target cells should not be discarded.

Why apparently redundant ATD and MLF pathways persist?

If the ATD and the MLF (abducens to medial rectus) connections were redundant, what forces have selected them during evolution? It is envisaged that the oldest form of eye movements is the vestibulo-ocular reflex that evolved to compensate for self-motion during locomotion (Walls 1962). Ondulatory swimming patterns in early vertebrates move the head from side to side, deteriorating thus proper image formation in the retina. Compensatory eye movements would cancel image deterioration. To achieve this, head velocity signals arising from the vestibular nerve are transmitted by second-order vestibular neurons towards their corresponding motoneurons. The excitatory pathways for the horizontal reflex have second-order neurons in the ATD which connect with medial rectus motoneurons, and medial vestibular nucleus projecting contralaterally to the abducens nucleus. Abducens internuclear neurons, in turn, project via the MLF to the contralateral medial rectus motoneurons (Straka and Baker 2013) in a likely redundant manner, since both ATD and abducens internuclear neurons contact the same medial rectus motoneuron pool. The abducens pathway via the MLF is already present in the lamprey (González et al. 1998) and it is conserved along vertebrates with the exception of elasmobranchs (Puzdrowski and Leonard 1994). It can be proposed that new overlapping functions have been selected for the maintenance of both pathways. Thus, during the course of evolution the MLF could have added new types of eye movements, such as saccades, fixations and vergence in its signaling properties (Delgado-García et al. 1986; Gamlin et al. 1989).

Lessons from lesions

The MLF lesions are the well-known source of internuclear ophthalmoplegia, causing some degree of paralysis of the adducting eye due to the loss of the internuclear abducens to medial rectus pathway. Tumors and vascular accidents have been the major sources of this syndrome, although there is

an increasing prevalence of myelin-related disorders, such as multiple sclerosis (Rotstein et al. 2018), that are also a common source of ophthalmoplegias and other vestibular-related deficits (Aw et al. 2017; Choi et al. 2017). Ocular symptoms help to the early diagnosis of these progressive diseases, whereas knowledge of the plastic and regenerative capabilities of these axonal tracts is of basic importance for prognosis and treatment.

Acknowledgements This work was supported by MICINN-FEDER Grant BFU2015-64515-P and PGC2018-094654-B-I00. RGH was a fellowship holder of the Universidad de Sevilla. Confocal microscopy was carried out at the Central Services of the Universidad de Sevilla (CITIUS).

Compliance with ethical standards

Conflict of interest Authors declare to have no conflict of interests.

Ethical approval All experimental procedures were in compliance with the European Union Directive on the protection of animals used for scientific purposes (2010/63/EU), and the Spanish legislation (RD 53/2013/BOE 34/11370-421).

References

Atwal JK, Massie B, Miller FD, Kaplan DR (2000) The TrkB-Shc site signals neuronal survival and local axon growth via MEK and PI3-kinase. Neuron 27:265–277. https://doi.org/10.1016/S0896-6273(00)00035-0

Aw ST, Chen L, Todd MJ, Barnett MH, Halmagyi GM (2017) Vestibulo-ocular reflex deficits with medial longitudinal fasciculus lesions. J Neurol 264:2119–2129. https://doi.org/10.1007/s00415-017-8607-8

Baker R, Highstein SM (1978) Vestibular projections to interno rectus subdivision of oculomotor nucleus. J Neurophysiol 41:1629–1646. https://doi.org/10.1152/jn.1978.41.6.1629

Bäurle J, Gorver BG, Grüsser-Cornehls U (1992) Plasticity of GABAergic terminals in Deiters' nucleus of weaver mutant and normal mice: a quantitative light microscope study. Brain Res 591:305–318. https://doi.org/10.1016/0006-8993(92)91712-N

Benítez-Temiño B, Morcuende S, Mentis GZ, de la Cruz RR, Pastor AM (2004) Expression of Trk receptors in the oculomotor system of the adult cat. J Comp Neurol 473:538–552. https://doi.org/10.1002/cne.20095

Biefang DC (1978) The course of direct projections from the abducens nucleus to the contralateral interno rectus subdivision of the oculomotor nucleus in the cat. Brain Res 145:277–289. https://doi.org/10.1016/0006-8993(78)90862-4

Bohlen MO, Warren S, May PJ (2017) A central mesencephalic reticular formation projection to medial rectus motoneurons supplying singly and multiply innervated extraocular muscle fibers. J Comp Neurol 525:2000–2018. https://doi.org/10.1002/cne.24187

Büttner-Ennever JA (2006) The extraocular motor nuclei: organization and functional neuroanatomy. In: Büttner-Ennever JA (ed) Neuroanatomy of the oculomotor system, progress in brain research, vol 151. Elveiser, Amsterdam, pp 95–126. https://doi.org/10.1016/s0079-6123(05)51004-5

Carpenter MB, Carleton SC (1983) Comparison of vestibular and abducens internuclear projections to the interno rectus subdivision of the oculomotor nucleus in the monkey. Brain Res 274:144–149. https://doi.org/10.1016/0006-8993(83)90530-9

Choi SY, Kim HJ, Kim JS (2017) Impaired vestibular responses in internuclear ophthalmoplegia: association and dissociation. Neurology 89:2476–2480. https://doi.org/10.1212/WNL.0000000000004745

Cohen-Cory S, Fraser SE (1995) Effects of brain-derived neurotrophic factor on optic axon branching and remodeling in vivo. Nature 378:192–196. https://doi.org/10.1038/378192a0

Cotman CW, Nadler JV (1978) Reactive synaptogenesis in the hippocampus. In: Cotman CW (ed) Neuronal plasticity. Raven, New York, pp 227–272

Cotman CW, Nieto-Sampedro M (1984) Cell biology of synaptic plasticity. Science 225:1287–1294. https://doi.org/10.1126/science.6382610

Cotman CW, Nieto-Sampedro M, Harris EW (1981) Synapse replacement in the nervous system of adult vertebrates. Physiol Rev 61:684–784. https://doi.org/10.1152/physrev.1981.61.3.684

Davis-López de Carrizosa MA, Morado-Díaz CJ, Tena JJ, Benítez-Temiño B, Pecero ML, Morcuende SR, de la Cruz RR, Pastor AM (2009) Complementary actions of BDNF and neurotrophin-3 on the firing patterns and synaptic composition of motoneurons. J Neurosci 29:575–587. https://doi.org/10.1523/JNEUROSCI.5312-08.2009

Davis-López de Carrizosa MA, Morado-Díaz CJ, Morcuende S, de la Cruz RR, Pastor AM (2010) Nerve growth factor regulates the firing patterns and synaptic composition of motoneurons. J Neurosci 30:8308–8319. https://doi.org/10.1523/JNEUROSCI.0719-10.2010

de la Cruz RR, Pastor AM, Martínez-Guijarro FJ, López-García C, Delgado-García JM (1992) Role of GABA in the extraocular motor nuclei of the cat: a postembedding immunocytochemical study. Neuroscience 5:911–929. https://doi.org/10.1016/0306-4522(92)90529-B

de la Cruz RR, Pastor AM, Martínez-Guijarro FJ, López-García C, Delgado-García JM (1998) Localization of parvalbumin, calretinin, and calbindin D-28k in identified extraocular motoneurons and internuclear neurons of the cat. J Comp Neurol 390:377–391. https://doi.org/10.1002/(SICI)1096-9861(19980119)390:3%3c377:AID-CNE6%3e3.0.CO;2-Z

Delgado-García JM, del Pozo F, Baker R (1986) Behavior of neurons in the abducens nucleus of the alert cat-II. Internuclear neurons. Neuroscience 17:953–973. https://doi.org/10.1016/0306-4522(86)90073-4

Dinocourt C, Gallagher SE, Thompson SM (2006) Injury-induced axonal sprouting in the hippocampus is initiated by activation of trkB receptors. Eur J Neurosci 24:1857–1866. https://doi.org/10.1111/j.1460-9568.2006.05067.x

Endo T, Spenger C, Tominaga T, Brene S, Olson L (2007) Cortical sensory map rearrangement after spinal cord injury: fMRI responses linked to Nogo signalling. Brain 130:2951–2961. https://doi.org/10.1093/brain/awm237

Federoff HJ, Grabczyk E, Fishman MC (1988) Dual regulation of GAP-43 gene expression by nerve growth factor and glucocorticoids. J Biol Biochem 263:19290–19295

Ferri CC, Ghasemlou N, Bisby MA, Kawaja MD (2002) Nerve growth factor alters p75 neurotrophin receptor-induced effects in mouse facial motoneurons following axotomy. Brain Res 950:180–185. https://doi.org/10.1016/S0006-8993(02)03035-4

Furuya N, Markham CH (1981) Arborization of axons in oculomotor nucleus identified by vestibular stimulation and intra-axonal injection of horseradish peroxidase. Exp Brain Res 43:289–303. https://doi.org/10.1007/BF00238370

Gallo G, Letourneau PC (1998) Localized sources of neurotrophins initiate axin collateral sprouting. J Neurosci 18:5403–5414. https://doi.org/10.1523/JNEUROSCI.18-14-05403.1998

Gamlin PD, Gnadt JW, Mays L (1989) Lidocaine-induced unilateral internuclear ophthalmoplegia: effects on convergence and conjugate eye movements. J Neurophysiol 62:82–95

Geremia NM, Pettersson LME, Hasmatali JC, Hryciw T, Danielsen N, Schreyer DJ, Valerie MK, Verge A (2010) Endogenous BDNF regulates induction of intrinsic neuronal growth programs in injured sensory neurons. Exp Neurol 223:128–142. https://doi.org/10.1016/j.expneurol.2009.07.022

Gomez-Pinilla F, Ying Z, Roy RR, Hodgson J, Edgerton VR (2004) Afferent input modulates neurotrophins and synaptic plasticity in the spinal cord. J Neurophysiol 92:3423–3432. https://doi.org/10.1152/jn.00432.2004

González MJ, Pombal MA, Rodicio MC, Anadón R (1998) Internuclear neurons of the ocular motor system of the larval sea lamprey. J Comp Neurol 401:1–15

Grinnell AD, Rheuben MB (1979) The physiology, pharmacology and trophic effectiveness of synapses formed by autonomic preganglionic nerves on frog skeletal muscle. J Physiol 289:219–240. https://doi.org/10.1113/jphysiol.1979.sp012734

Hernández RG, Benítez-Temiño B, Morado-Díaz CJ, Davis-López de Carrizosa MA, de la Cruz RR, Pastor AM (2017a) Effects of selective deafferentation on the discharge characteristics of medial rectus motoneurons. J Neurosci 37:9172–9188. https://doi.org/10.1523/JNEUROSCI.1391-17.2017

Hernández RG, Silva-Hucha S, Morcuende S, de la Cruz RR, Pastor AM, Benítez-Temiño B (2017b) Extraocular motor system exhibits a higher expression of neurotrophins when compared with other brainstem motor systems. Front Neurosci 11:399. https://doi.org/10.3389/fnins.2017.00399

Highstein SM, Baker R (1978) Excitatory termination of abducens internuclear neurons on medial rectus motoneurons: relationship to syndrome of internuclear ophthalmoplegia. J Neurophysiol 41:1647–1661. https://doi.org/10.1152/jn.1978.41.6.1647

Highstein SM, Holstein GR (2006) The anatomy of the vestibular nuclei. In: Büttner-Ennever JA (ed) Neuroanatomy of the oculomotor system, progress in brain research, vol 151. Elsevier, Amsterdam, pp 157–203. https://doi.org/10.1016/s0079-6123(05)51006-9

Him A, Dutia MB (2001) Intrinsic excitability changes in vestibular nucleus neurons after unilateral deafferentation. Brain Res 908:58–66. https://doi.org/10.1016/S0006-8993(01)02600-2

Inoue A, Sanes JR (1997) Lamina-specific connectivity in the brain: regulation by *N*-cadherin, neurotrophins and glycoconjugates. Science 276:1428–1431. https://doi.org/10.1126/science.276.5317.1428

Izawa Y, Sugiuchi Y, Shinoda Y (1999) Neural organization from the superior colliculus to motoneurons in the horizontal oculomotor system of the cat. J Neurophysiol 81:2597–2611

Jakeman LB, Wei P, Guan Z, Stokes BT (1998) Brain-derived neurotrophic factor stimulates hindlimb stepping and sprouting of cholinergic fibers after spinal cord injury. Exp Neurol 154:170–184. https://doi.org/10.1006/exnr.1998.6924

Johnson RA, Okragly AJ, Haak-Frendscho M, Mitchell GS (2000) Cervical dorsal rhizotomy increases brain-derived neurotrophic factor and neurotrophin-3 expression in the ventral spinal cord. J Neurosci 20:1–5. https://doi.org/10.1523/JNEUROSCI.20-10-j0005.2000

Keast JR, Kepper ME (2001) Differential regulation of TrkA and p75 in noradrenergic pelvic autonomic ganglion cells after deafferentation of their cholinergic neighbours. Eur J Neurosci 13:211–220. https://doi.org/10.1111/j.1460-9568.2001.01374.x

Krassioukov AV, Weaver LC (1996) Morphological changes in sympathetic preganglionic neurons after spinal cord injury in rats. Neuroscience 1:211–225. https://doi.org/10.1016/0306-4522(95)00294-S

Lee KS, Stanford EJ, Cotman CW, Lynch GS (1977) Ultrastructural evidence for bouton proliferation in the partially deafferented dentate gyrus of the adult rat. Exp Brain Res 29:475–485. https://doi.org/10.1007/BF00236185

Lindsay RM (1994) Trophic protection of motor neurons: clinical potential in motor neuron diseases. J Neurol 242:S8–S11. https://doi.org/10.1007/BF00939232

Lund RD, Lund JS (1971) Modifications of synaptic patterns in the superior colliculus of the rat during development and following deafferentation. Vision Res Suppl 3:281–298. https://doi.org/10.1016/0042-6989(71)90046-0

Masliah E, Fagan AM, Terry RD, DeTeresa R, Mallory M, Gage FH (1991) Reactive synaptogenesis assessed by synaptophysin immunoreactivity is associated with GAP-43 in the dentate gyrus of the adult rat. Exp Neurol 113:131–142. https://doi.org/10.1016/0014-4886(91)90169-D

Matthews DA, Cotman C, Lynch G (1976) An electron microscopic study of lesion-induced synaptogenesis in the dentate gyrus of the adult rat. II. Reappearance of morphologically normal synaptic contacts. Brain Res 115:23–41. https://doi.org/10.1016/0006-8993(76)90820-9

McCrea RA, Baker R (1985) Anatomical connections of the nucleus prepositus of the cat. J Comp Neurol 237:377–407

Mendell LM, Sassoon EM, Wall PD (1978) Properties of synaptic linkage form long-ranging afferents onto dorsal horn neurons in normal and deafferented cats. J Physiol 285:299–310. https://doi.org/10.1113/jphysiol.1978.sp012572

Mohiuddin L, Fernandez K, Tomlinson DR, Fernyhough P (1995) Nerve growth factor and neurotrophin-3 enhance neurite outgrowth and up-regulate the levels of messenger RNA for growth-associated protein GAP-43 and Tal a-tubulin in cultured adult rat sensory neurons. Neurosci Lett 185:20–23. https://doi.org/10.1016/0304-3940(94)11215-5

Morcuende S, Matarredona ER, Benítez-Temiño B, Muñoz-Hernández R, Pastor AM, de la Cruz RR (2011) Differential regulation of the expression of neurotrophin receptors in rat extraocular motoneurons after lesion. J Comp Neurol 519:2335–2352. https://doi.org/10.1002/cne.22630

Morcuende S, Muñoz-Hernández R, Benítez-Temiño B, Pastor AM, de la Cruz RR (2013) Neuroprotective effects of NGF, BDNF, NT-3 and GDNF on axotomized extraocular motoneurons in neonatal rats. Neuroscience 250:31–48. https://doi.org/10.1016/j.neuroscience.2013.06.050

Nadler JV, Perry BW, Cotman CW (1980a) Selective reinnervation of hippocampal area CA1 and the fascia dentata after destruction of CA3-CA4 afferents with kainic acid. Brain Res 182:1–9. https://doi.org/10.1016/0006-8993(80)90825-2

Nadler JV, Perry BW, Gentry C, Cotman CW (1980b) Loss and reacquisition of hippocampal synapses after selective destruction of CA3-CA4 afferents with kainic acid. Brain Res 191:387–403. https://doi.org/10.1016/0006-8993(80)91289-5

Nguyen LT, Spencer RF (1999) Abducens internuclear and ascending tract of Deiters inputs to medial rectus motoneurons in the cat oculomotor nucleus: neurotransmitters. J Comp Neurol 411:73–86. https://doi.org/10.1002/(SICI)1096-9861(19990816)411:1%3c73:AID-CNE6%3e3.0.CO;2-7

Nguyen LT, Baker R, Spencer RF (1999) Abducens internuclear and ascending tract of Deiters inputs to medial rectus motoneurons in the cat oculomotor nucleus: synaptic organization. J Comp Neurol 405:141–159. https://doi.org/10.1002/(SICI)1096-9861(19990308)405:2%3c141:AID-CNE1%3e3.0.CO;2-%23

Nja A, Purves D (1978) The effects of nerve growth factor and its antiserum on synapses in the superior cervical ganglion of the guinea pig. J Physiol 277:53–75. https://doi.org/10.1113/jphysiol.1978.sp012260

Paxinos G, Watson C (2009) The rat brain in stereotaxic coordinates. Elsevier, Amsterdam

Perrone-Bizzozero NI, Neve RL, Irwin N, Lewis S, Fischer I, Benowitz LI (1991) Post-transcriptional regulation of GAP-43 mRNA levels during neuronal differentiation and nerve regeneration. Mol Cell Neurosci 2:402–409. https://doi.org/10.1016/1044-7431(91)90027-L

Perrone-Bizzozero NI, Cansino VV, Kohn DT (1993) Posttranscriptional regulation of GAP-43 gene expression in PC12 cells through protein kinase C-dependent stabilization of the mRNA. J Cell Biol 120:1263–1270. https://doi.org/10.1083/jcb.120.5.1263

Puzdrowski RL, Leonard RB (1994) Vestibulo-oculomotor connections in an elasmobranch fish, the Atlantic stingray, *Dasyatis sabina*. J Comp Neurol 339:587–597

Reisine H, Highstein SM (1979) The ascending tract of Deiters' conveys a head velocity signal to medial rectus motoneurons. Brain Res 170:172–176. https://doi.org/10.1016/0006-8993(79)90949-1

Reisine H, Strassman A, Highstein SM (1981) Eye position and eye velocity signals are conveyed to medial rectus motoneurons in the alert cat by the ascending tract of Deiters'. Brain Res 211:153–157. https://doi.org/10.1016/0006-8993(81)90075-5

Rotstein DL, Chen H, Wilton AS, Kwong JC, Marrie RA, Gozdyra P, Krysko KM, Kopp A, Copes R, Tu K (2018) Temporal trends in multiple sclerosis prevalence and incidence in a large population. Neurology 90:e1435–e1441. https://doi.org/10.1212/wnl.0000000000005331

Ruit KG, Snider WD (1991) Administration or deprivation of nerve growth factor during development permanently alters neuronal geometry. J Comp neurol 314:106–131. https://doi.org/10.1002/cne.903140110

Sanna MD, Ghelardini C, Galeotti N (2017) HuD-mediated distinct BDNF regulatory pathways promote regeneration after nerve injury. Brain Res 1659:55–63. https://doi.org/10.1016/j.brainres.2017.01.019

Scott AL, Borisoff JF, Ramer MS (2005) Deafferentation and neurotrophin-mediated intraspinal sprouting: a central role for the p75 neurotrophin receptor. Eur J Neurosci 21:81–92. https://doi.org/10.1111/j.1460-9568.2004.03838.x

Sedivec MJ, Ovelmen-Levitt J, Karp R, Mendell LM (1983) Increase in nociceptive input to spinocervical tract neurons following chronic partial deafferentation. J Neurosci 3:1511–1519. https://doi.org/10.1523/JNEUROSCI.03-07-01511.1983

State FA, Dessouky HI (1977) Effect of length of the distal stump of transected nerve upon the rate of degeneration of taste buds. Acta Anat 98:353–360. https://doi.org/10.1159/000144812

Straka H, Baker R (2013) Vestibular blueprint in early vertebrates. Front Neural Circuits 7:182. https://doi.org/10.3389/fncir.2013.00182

Tessler A, Glazer E, Artymyshyn R, Murray M, Goldberger ME (1980) Recovery of substance P in the cat spinal cord after unilateral lumbosacral deafferentation. Brain Res 191:459–470. https://doi.org/10.1016/0006-8993(80)91294-9

Walls GL (1962) The evolutionay history of eye movements. Vision Res 2:69–80

Zhang Y, Gamlin PD, Mays LE (1991) Antidromic identification of midbrain near response cells projecting to the oculomotor nucleus. Exp Brain Res 84:525–528

Zhang B, Goldberger ME, Wu LF, Murray M (1995) Plasticity of complex terminals in lamina II in partially deafferented spinal cord: the cat spared root preparation. Exp Neurol 132:186–193. https://doi.org/10.1016/0014-4886(95)90024-1